

# Raman Spectroscopy Vibrational Analysis of Octahedrally Coordinated Fluorides: Application to Transition Metal Fluoride Glasses

B. BOULARD AND C. JACOBONI

*Laboratoire des Fluorures, UA CNRS 449, Faculté des Sciences, Université du Maine, 72017 Le Mans Cedex, France*

AND M. ROUSSEAU

*Laboratoire de Physique de l'Etat Condensé, UA CNRS 807, Faculté des Sciences, Université du Maine, 72017 Le Mans Cedex, France*

Received August 29, 1988; in revised form January 27, 1989

An extensive Raman investigation of octahedrally coordinated single-crystal fluorides have been performed. The theoretical study of these phases, using group theory, gives the evidence of close relationship between metal oxidation number, connection schemes, and spectra features. The results of this study, when applied to the case of transition metal fluoride glasses, propose these glasses to be built up with octahedral entities predominantly linked by corners to form one-dimensional networks. © 1989 Academic Press, Inc.

## Introduction

Fluoride glasses belong to a new class of materials with high potentiality for fiber optics because of their ultra transparency in the middle infrared and a very low estimated loss value (about  $10^{-3}$  dB/km at 2.55  $\mu\text{m}$ ) (1, 2).

Three-dimensional (3d) transition metal fluoride glasses (TMFG) have been extensively investigated in various fields (X-ray and neutron diffraction (3-5); EXAFS (6, 7), NMR (8), magnetism (9)) to get coherent crystal chemistry knowledge.

Raman spectroscopy seems to be another way to access the structure of these materials. With a large number of single crystals of octahedrally coordinated 3d transition metals in various known structural types

we looked at correlations between the vibration modes and the oxidation number and/or the connection scheme. These data were used to interpret the Raman spectra of the fluoride glasses (TMFG) which contain the same entities.

## I. Experimental Procedures

### 1. Sample Preparations

Crystalline samples were obtained either from a chloride flux method (10) ( $\text{Na}_5\text{Al}_3\text{F}_{14}$ ,  $\text{Cs}_2\text{NaAl}_3\text{F}_{12}$ ,  $\text{Rb}_2\text{CrF}_5$ ,  $\text{CoF}_2$ ,  $\text{MnF}_2$ ,  $\text{NaMnCrF}_6$ ,  $\beta\text{-AlF}_3$ ,  $\text{K}_2\text{NaGaF}_6$ ) or HF hydrothermal synthesis (11) ( $(\text{NH}_4)_3\text{AlF}_6$ ,  $\text{Tl}_2\text{AlF}_5 \cdot \text{H}_2\text{O}$ ,  $\text{TlAlF}_4$ ,  $\text{KAlF}_4$ ,  $\beta\text{-RbAlF}_4$ ).

Bulk glass samples are prepared as already described (12) (by melting the mix-

ture of anhydrous fluorides in a platinum crucible; the melt is quenched on a pre-heated brass mold); they are then polished with  $\text{OH}^-$  free solvent.

## 2. Raman Measurements

Raman spectra were recorded with a DILOR Z24 spectrometer (triple monochromator, photon counting electronics); 514.5- and 457.9-nm lines of an Argon-ion laser (Coherent INOVA 90) have been used as the excitation source.

Single-crystal Raman spectra were recorded under a microscope (ULF  $\times 50$  objective) from 20 to  $600\text{ cm}^{-1}$  with  $700\text{-}\mu\text{m}$  slit width. Although imperfectly defined under the microscope, polarization effects may be qualitatively taken into account. The intensities of all the Raman spectra are given with arbitrary units; a typical polarized Raman spectrum is shown in Fig. 1.

The measurements for TMFG were carried out on large polished samples in the  $90^\circ$  scattering configuration in both the polarized H-H configuration (the scattered light

is analyzed for electric vector parallel to that of the incident radiation) and the H-V configuration (electric vector perpendicular to incident light).

## II. Vibrational Study of Crystalline Fluorides

### 1. Crystal Structures of Studied Phases

The most important features of their crystal chemistry are described in the following lines.

(a) *Isolated octahedra.* The  $Fm3m$  cubic structure of  $(\text{NH}_4)_3\text{AlF}_6$  (13) or elpasolite,  $\text{K}_2\text{NaGaF}_6$  (14), is shown in Fig. 2.

(b) *One-dimensional network structures.* Two examples of structures built up from isolated chains of corner-shared octahedra ( $\text{Ti}_2\text{AlF}_5 \cdot \text{H}_2\text{O}$  (15) *trans*-chains and  $\text{Rb}_2\text{CrF}_5$  (16) *cis*-chains) are shown in Figs. 3 and 4, respectively.

(c) *Two-dimensional network structures.* In the fluoroaluminate case, we can distinguish two kinds of  $(\text{AlF}_4)_n$  layers:

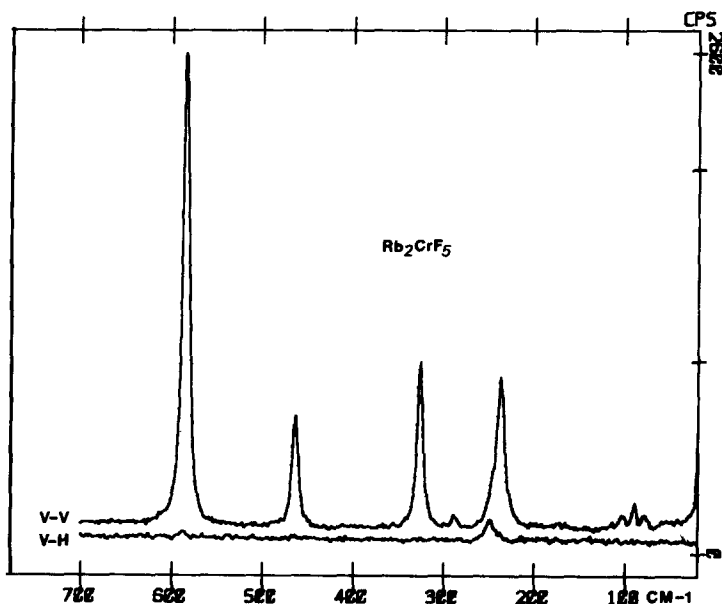
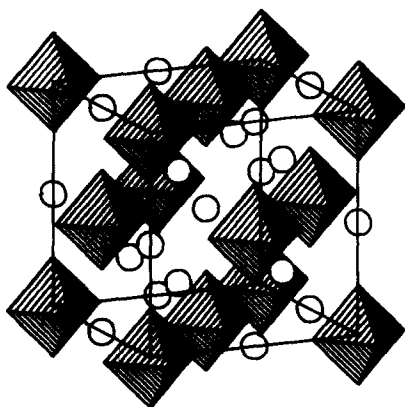


FIG. 1. Polarized Raman spectrum of  $\text{Rb}_2\text{CrF}_5$ .

FIG. 2.  $Fm\bar{3}m$  structure of  $(NH_4)_3AlF_6$ .

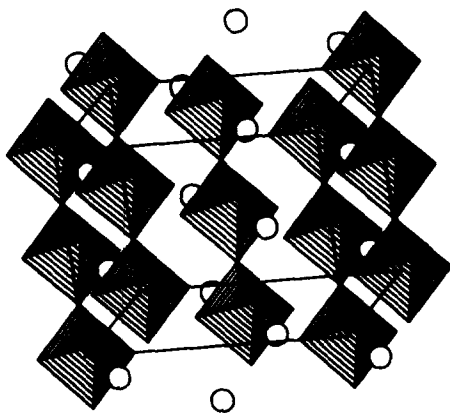
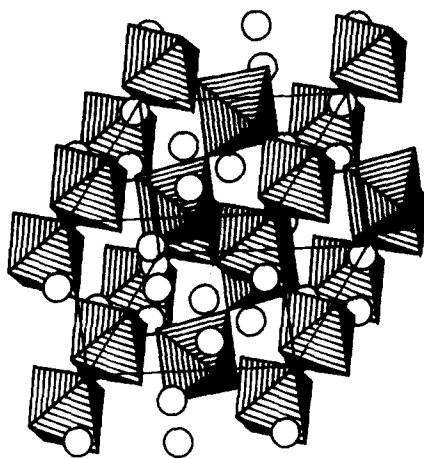
—tetragonal as in  $TlAlF_4$  (17) (Fig. 5) with its isotypes  $KAlF_4$  (17) and  $\beta$ - $RbAlF_4$  (18), or in  $Na_5Al_3F_{14}$  (19) (Fig. 6);

—hexagonal as in hexagonal tungsten bronze (H.T.B.)-type  $Cs_2NaAl_3F_{12}$  (20) (Fig. 7).

(d) *Tridimensional structures.* Various structural types were studied:

—The rutile structure has edge-shared chains of octahedra linked together by corners as in  $CoF_2$ ,  $MnF_2$  (21) (Fig. 8).

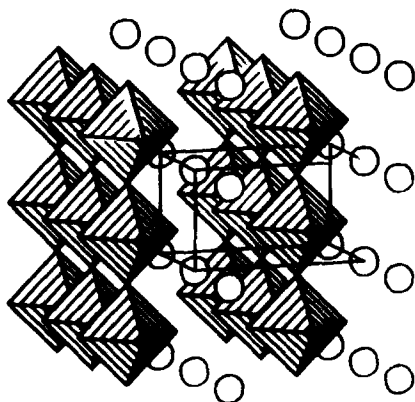
—The H.T.B.-type  $\beta$ - $AlF_3$  (22) is shown in Fig. 9.

FIG. 3. Structure of  $Rb_2AlF_5 \cdot H_2O$ . The octahedra are *trans*-connected.  $\circ$ ,  $H_2O$  molecules.FIG. 4. Structure of  $Rb_2CrF_5$ ; the octahedra are *cis*-connected.

—The  $NaMnCrF_6$  (23) structure (Fig. 10) has octahedra linked by corners and by edges with two different oxidation number cations ( $Mn^{2+}$  and  $Cr^{3+}$ ).

## 2. Discussion

(1) *Evidence of pure symmetric stretching (SS).* Raman spectroscopic studies performed on  $AAlF_4$  ( $A = K, Rb, Cs, NH_4$ ) compounds show that the  $A_{1g}$  band (VV polarized) of the Raman active vibrations of  $AlF_6^{3-}$  octahedron lies in the range

FIG. 5. Structure of  $TlAlF_4$ .

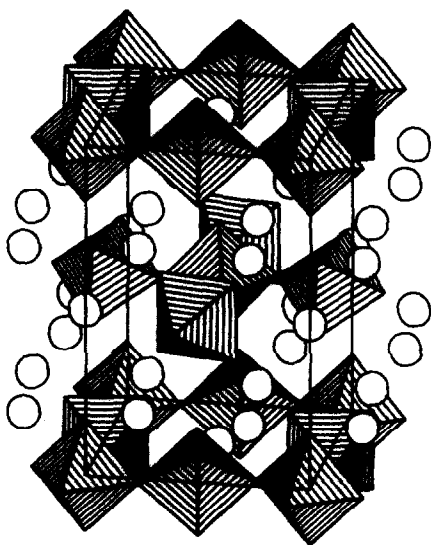


FIG. 6. Structure of  $\text{Na}_3\text{Al}_3\text{F}_{14}$  showing  $[\text{Al}_3\text{F}_{14}]_n^{5n-}$  sheets.

$515\text{--}545\text{ cm}^{-1}$ . Lattice dynamics calculations unambiguously show that this band is assigned to the symmetric stretching (SS) of the nonbridging F atoms  $F_{\text{nb}}$  (24, 25); it is

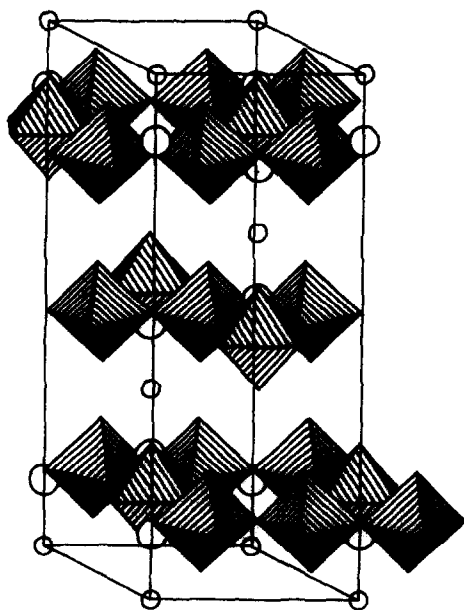


FIG. 7. Structure of  $\text{Cs}_2\text{NaAl}_3\text{F}_{12}$ ; Al atoms form triangular and hexagonal rings.

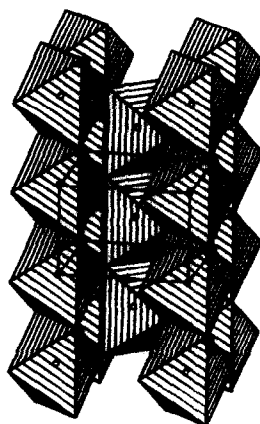


FIG. 8. Rutile structure.

the case for crystals with isolated octahedra or mono and bidimensional networks.

Figure 11 shows the Raman spectra obtained for  $\text{K}_2\text{NaGaF}_6$ ,  $\text{Tl}_2\text{AlF}_5 \cdot \text{H}_2\text{O}$ , and  $\text{Cs}_2\text{NaAl}_3\text{F}_{12}$ .

According to Rousseau *et al.* (26), when neglecting F-F interactions, the harmonic force constant associated with the motion of F atoms in the  $M\text{--}F$  direction of  $\text{MF}_6$  octahedron may be written in the form

$$K_{\text{F}\parallel} = \frac{e^2}{16r^3} (2A_2 - \alpha Z_M Z_F), \quad (1)$$

where  $Z_M$  and  $Z_F$  are the formal ionic charge of respective ions,  $r$  is their distance,  $A_2$  is a parameter characteristic of the  $M\text{--}F$  short-range interaction, and  $\alpha$  is a geometric constant.

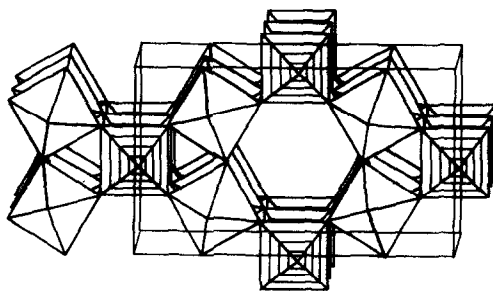


FIG. 9. Structure of  $\beta\text{-AlF}_3$ .

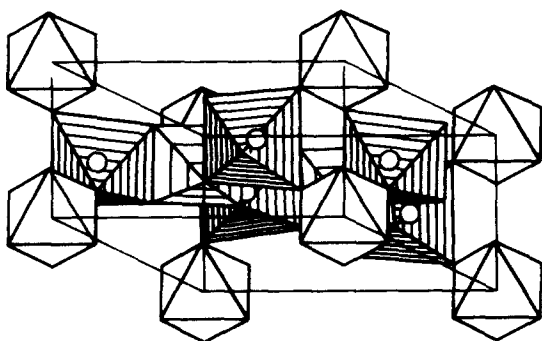


FIG. 10. Structure of  $\text{NaMnCrF}_6$ .  $\text{CrF}_6$  and  $\text{MnF}_6$  share both edges and corners.

Furthermore, the minimization of the total energy provides a relation between  $A_2$  and the ionic charges:  $A_2 \propto Z_M Z_F$ . Thus, the harmonic force constant is proportional to  $Z_M Z_F$  and  $r^{-3}$ . The frequency of the SS vibration may be expressed by

$$\omega_{\text{SS}}^2 = \frac{K \cdot e^2 \cdot Z_M Z_F}{m_F r^3} \quad (2)$$

When neglecting the  $r^{-3}$  dependence  $\omega_{\text{SS}}$  is roughly proportional to  $Z_M^{1/2}$ . As previously outlined  $520 \text{ cm}^{-1}$  is the order of magnitude of  $\omega_{\text{SS}}$  for  $F_{\text{nb}}$  vibrations in  $\text{MF}_6$  octahedra for  $M^{3+}$  ions ( $Z_M = 3$ ). Then, we can estimate  $\omega_{\text{SS}}$  as 600 and  $420 \text{ cm}^{-1}$  for  $\text{MF}_6$  octahedra with  $M^{4+}$  and  $M^{2+}$  ions, respectively.

TABLE I  
OBSERVED VIBRATION FREQUENCY AND MEAN  $M$ - $F$   
DISTANCE (X-RAY DATA)

| Cation           | Crystal  | Frequency<br>( $\text{cm}^{-1}$ ) | $M$ - $F$<br>( $\text{\AA}$ ) | Octahedral<br>network |
|------------------|--|-----------------------------------|-------------------------------|-----------------------|
| $\text{Zr}^{4+}$ | $\text{Li}_2\text{ZrF}_6$ (27)                     | 585                               | 2.016                         | Isolated              |
|                  | $\text{Cs}_2\text{ZrF}_6$ (27)                     | 577                               | 2.112                         | Isolated              |
| $\text{Ga}^{3+}$ | $\text{K}_2\text{NaGaF}_6$                         | 558                               | 1.940                         | Isolated              |
| $\text{Al}^{3+}$ | $(\text{NH}_4)_3\text{AlF}_6$                      | 546                               | 1.900                         | Isolated              |
|                  | $\text{K}_3\text{AlF}_5 \cdot \text{H}_2\text{O}$  | 536                               | 1.908                         | One dim.              |
|                  | $\text{Rb}_2\text{AlF}_5 \cdot \text{H}_2\text{O}$ | 530                               | 1.908                         | One dim.              |
|                  | $\text{Ti}_2\text{AlF}_5 \cdot \text{H}_2\text{O}$ | 516                               | 1.908                         | One dim.              |
|                  | $\text{Cs}_2\text{NaAl}_3\text{F}_{12}$            | 536                               | 1.801                         | Two dim.              |
|                  | $\text{Na}_2\text{Al}_3\text{F}_{14}$              | 534                               | 1.790                         | Two dim.              |
|                  | $\text{TiAlF}_4$                                   | 520                               | 1.784                         | Two dim.              |
|                  | $\text{KAlF}_4$                                    | 545                               | 1.784                         | Two dim.              |
| $\text{Cr}^{3+}$ | $\beta$ - $\text{RbAlF}_4$                         | 528                               | 1.808                         | Two dim.              |
|                  | $\text{Na}_5\text{Cr}_3\text{F}_{14}$              | 544                               | 1.840                         | Two dim.              |

In fact, as shown in Table I, strong  $A_{1g}$  bands are observed in the predicted frequency range for many compounds built with  $\text{MF}_6$  octahedra on  $M^{4+}$  and  $M^{3+}$  ions.

The last approximation allows us to identify one of the totally symmetric Raman lines as corresponding to SS of  $\text{MF}_6$  octahedra.

In order to go further we reported in Fig. 12  $\Gamma = \omega_{\text{SS}} \cdot r^{3/2} \cdot Z_M^{-1/2}$  as a function of the degree of connectivity between the octahedra. Figure 12 clearly shows that  $\omega_{\text{SS}}$  increases when the degree of connectivity decreases. This variation may be attributed to modifications of F-F short-range interactions. Effectively, in two-dimensionally connected octahedra the "SS" vibration involves only two nonbridging  $F_{\text{nb}}$  atoms; on the other hand, in-phase motion of four  $F_{\text{nb}}$  atoms occurs in compounds with one-dimensionally connected octahedra. As illustrated in Fig. 13, the correlated motion of  $F_{\text{nb}}$  atoms enhances the F-F interatomic distance variations leading to an increase of the short-range F-F force constant. This effect is doubled in the case of isolated octahedra where 6  $F_{\text{nb}}$  atoms are moving simultaneously.

The motion of both  $M^{3+}$  and  $F^-$  ions in stretching mode should lead to higher frequencies: the reduced mass  $1/m_F$  in Eq. (2) is replaced by  $1/m_F + 1/m_{\text{Cr}}$  in the  $\text{Rb}_2\text{CrF}_5$  case; the group theory shows that the  $A_g$  modes ( $D_{2h}$ ) involve motion of both  $\text{Cr}^{3+}$  and  $F^-$  ions; the observed frequency ( $584 \text{ cm}^{-1}$ ) is consistent with precedent remarks.

Apart from the SS mode involving nonbridging  $F_{\text{nb}}$  atoms (noted  $\nu^{\text{S}}$  in Almeida's work (28)), there exists a symmetric bending (SB) mode involving motion of bridging fluorine atoms  $F_b$  (noted  $\omega_{\text{SS}}$  in the same work) (Fig. 14). According to Almeida, the frequency  $\omega_{\text{SB}}$  of the SB vibration of  $F_b$  atoms is related to the frequency  $\omega_{\text{SS}}$  of  $F_{\text{nb}}$  atoms by

$$\omega_{\text{SB}}^2 = 2 \cdot \omega_{\text{SS}}^2 \cdot \cos^2 \theta/2. \quad (3)$$

This last expression has been derived using nearest-neighbor central forces between  $M$  and  $F$  atoms; in fact, when plotting  $\omega$  versus  $\cos \theta/2$  for various compounds (respec-

tively  $Tl_2AlF_5 \cdot H_2O$ ,  $K_2AlF_5 \cdot H_2O$ ,  $Rb_2AlF_5 \cdot H_2O$ ,  $Na_5Al_3F_{14}$ ,  $\beta-AlF_3$ , and  $Cs_2NaAl_3F_{12}$ , Fig. 15) with small variations of Al-F distances ( $\Delta r/r < 0.5\%$ ), it appears that

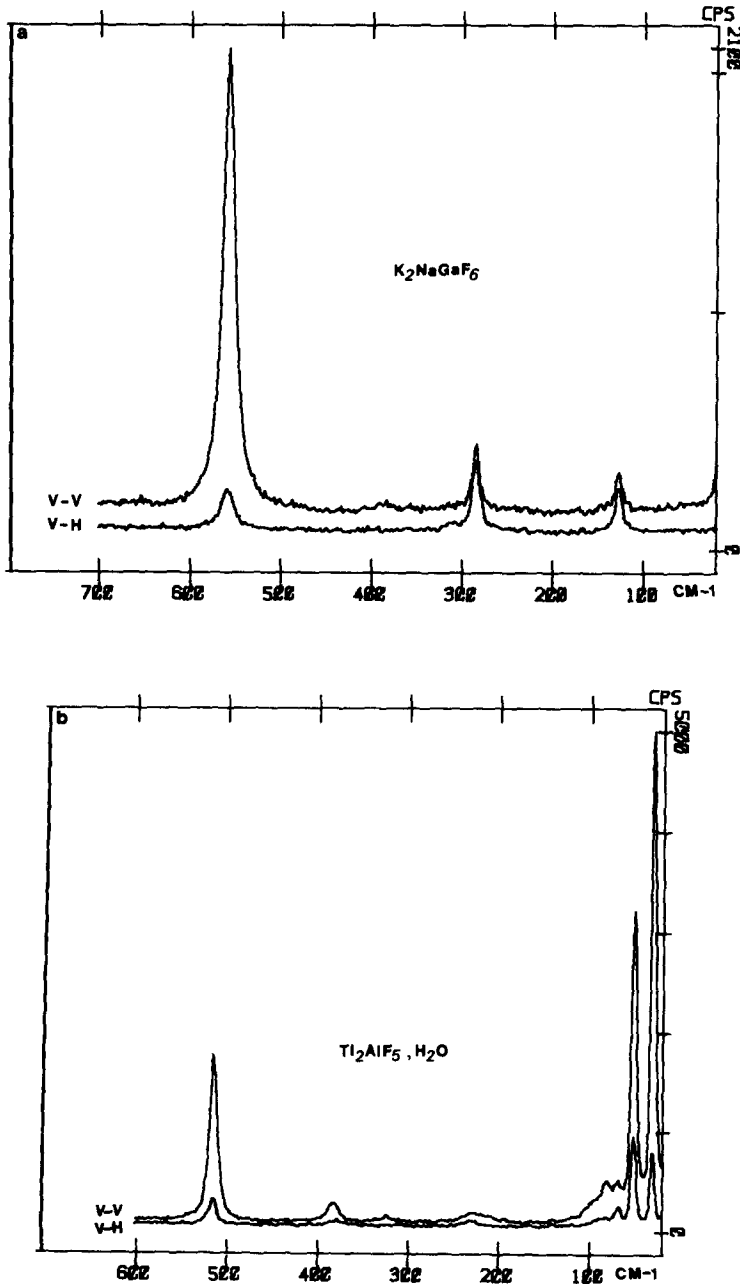


FIG. 11. Polarized Raman spectra of  $K_2NaGaF_6$  (a),  $Tl_2AlF_5 \cdot H_2O$  (b), and  $Cs_2NaAl_3F_{12}$  (c).

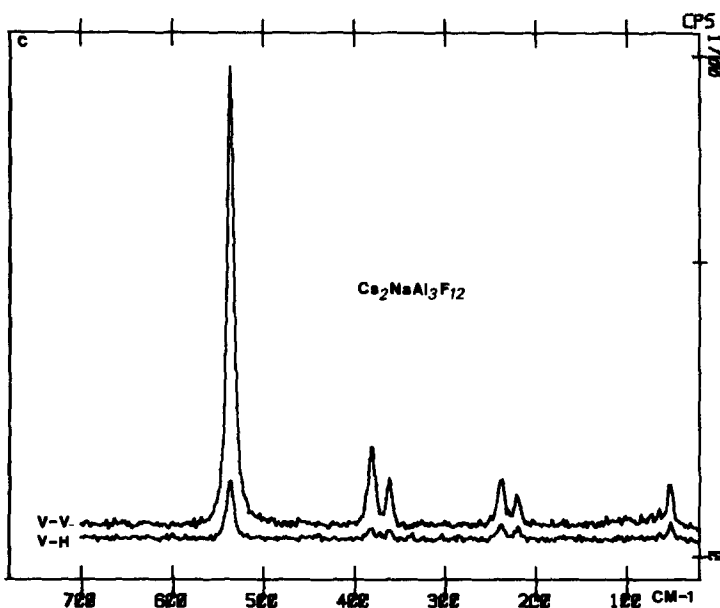


FIG. 11-Continued

the following law is much more realistic.

$$\omega_{SB} = A + B \cdot \cos \theta/2, \quad (4)$$

where  $A$  characterizes interactions other than  $M-F$  ones and  $B$  is estimated to be  $514 \text{ cm}^{-1}$ . The difference between  $B$  and

$\omega_{SS} \sqrt{2}$  ( $735 \text{ cm}^{-1}$ ) gives an order of magnitude of the contribution of noncentral forces. It is noteworthy that  $A$  represents the symmetric bending frequency in the case of  $\theta = 180^\circ$ . This situation occurs in the high-temperature phase of  $\text{RbAlF}_4$  where, according to Bulou (29), the corresponding  $X_7^2$  zone boundary mode is observed at  $256 \text{ cm}^{-1}$  in agreement with the

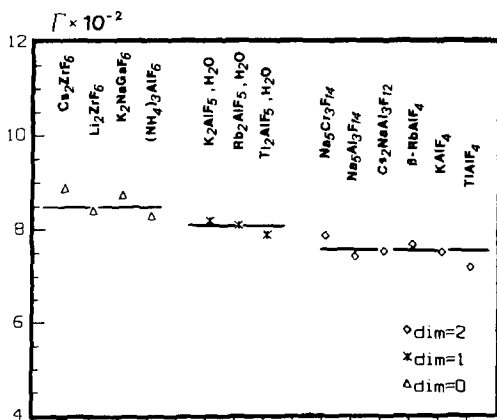


FIG. 12. Variation of connecting scheme criterion  $\Gamma = r^{3/2}\omega/\sqrt{q}$  with degree of connectivity.

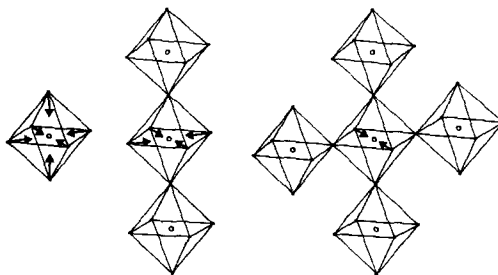


FIG. 13.  $F^-$  motion in  $SS A_{1g}$  mode for isolated octahedra, one-dimensional and two-dimensional networks. When more  $F^-$  anions are involved,  $F-F$  short-range interactions increase leading to a higher symmetric stretching frequency  $\omega_{SS}$ .

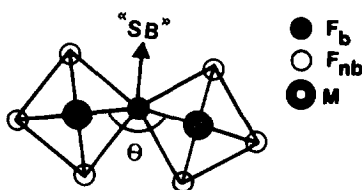


FIG. 14. Schematic illustration of the symmetric bending SB vibration of bridging fluorine atom  $F_b$ .

$232 \text{ cm}^{-1}$  extrapolated from our measurements.

(2) *Case of tridimensional structures.* All of the previously mentioned crystals display a symmetric stretching  $A_{1g}$  Raman line involving elongation of  $M-F_{nb}$  bonds. The frequency of this SS mode depends mainly on the oxidation number of metal  $M$  and on the degree of connectivity of the  $MF_6$  octahedra. The interpretation of this particular line was justified by both lattice dynamics calculation and symmetry determination (25) of the Brillouin zone center normal mode with group theory. In the case of tridimensional networks (without  $F_{nb}$ ), each structure has to be seen as a special case.

Figure 16 shows the Raman spectra of  $\text{CoF}_2$ ,  $\beta\text{-AlF}_3$ , and  $\text{NaMnCrF}_6$ :

(1) In the two  $\text{AlF}_3$  forms, symmetry does not allow any Raman-active SS modes of  $M-F$  bonds; as expected, the characteristic SS line is not found.

(2) The rutile structure ( $\text{MnF}_2$ ,  $\text{CoF}_2$ ) is built with both corner and edge sharing of  $MF_6$  octahedra; nevertheless, as shown in Table II, the observed frequencies for  $A_{1g}$  mode are in the same range as the  $\omega_{SS}$  value.

(3) The  $\text{NaMnCrF}_6$  spectrum shows three lines at  $572$ ,  $538$ , and  $358 \text{ cm}^{-1}$ ; the first two lines are consistent with the existence of two different crystallographic sites for  $\text{Cr}^{3+}$ . One  $\text{Cr}_1$  (2d) participates in the  $A_{1g}$  vibration mode, giving a higher vibration at  $572 \text{ cm}^{-1}$  (this case is to be compared to the case of  $\text{Rb}_2\text{CrF}_5$ ); the other  $\text{Cr}_2$  (1a) has no active Raman mode: the  $538 \text{ cm}^{-1}$  line can be attributed to the  $\omega_{SS}$  vibration mode.

Since  $\text{NaMnCrF}_6$  has a three-dimensional network involving  $\text{Cr-F-Mn}$  junctions, we could have expected the  $\omega_{SS}$  vibration to be perturbed by  $\text{Mn}^{2+}$ ; this effect

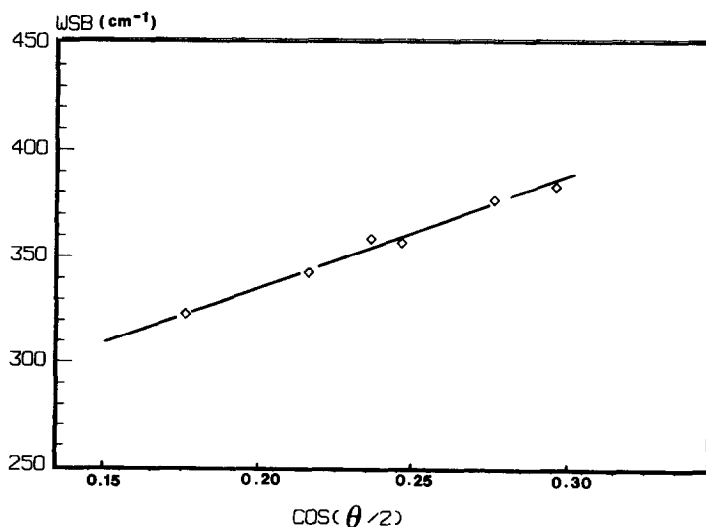


FIG. 15. Variation of symmetric bending mode frequency  $\omega_{SB}$  versus  $\cos \theta/2$ , where  $\theta$  is the  $M-F-M$  angle defined in Fig. 14.



TABLE II  
OBSERVED VIBRATION FREQUENCY FOR THE  $A_{1g}$   
MODE AND MEAN  $M-F$  DISTANCE (X-RAY DATA)

| Cation           | Crystal            | Frequency<br>( $\text{cm}^{-1}$ ) | $M-F$<br>( $\text{\AA}$ ) |
|------------------|--------------------|-----------------------------------|---------------------------|
| $\text{Cr}^{3+}$ | $\text{NaMnCrF}_6$ | 538–572                           | 1.909                     |
| $\text{Mn}^{2+}$ | $\text{NaMnCrF}_6$ | 358                               | 2.130                     |
|                  | $\text{MnF}_2$     | 338                               |                           |
| $\text{Co}^{2+}$ | $\text{CoF}_2$     | 364                               | 2.076                     |

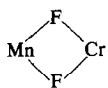
is not observed. The  $538 \text{ cm}^{-1}$  frequency very well agrees with values found in Table I. We explain this result by easily distorted  $\text{MnF}_6$  octahedra; the distortion is consistent with the known behavior of  $M^{2+}$  ions as connecting agents in fluoride glass systems.

The  $358 \text{ cm}^{-1}$  line corresponds both to  $M^{\text{II}}-F$  ( $\omega_{\text{SS}}$ ) vibration and to  $M^{\text{III}}\text{F}_6$  distortion (24, 25) because of the edge sharing of  $M^{\text{II}}\text{F}_6$  and  $M^{\text{III}}\text{F}_6$  octahedra. Table III compares observed and calculated frequencies of symmetric bending modes  $\omega_{\text{SB}}$ , using an expression derived from Eq. (3):

$$\omega_{\text{SB}}^2 = [\omega_{\text{SS}}^2(M^{\text{II}}) + \omega_{\text{SS}}^2(M^{\text{III}})]/\cos^2 \theta/2. \quad (5)$$

A fairly good agreement is found for Mn–F–Cr bending where octahedra share corners (262/258), this is not the case when octahedra share edges (404/358): either Eq. (2) is not valid for this particular configuration or edge Mn–F–Cr vibration does not occur.

TABLE III  
COMPARISON OF OBSERVED AND CALCULATED  
FREQUENCIES OF SYMMETRIC BENDING MODES  $\omega_{\text{SB}}$

| Crystal  | Bond  | $\theta$ ( $^\circ$ ) | $\omega_{\text{calc}}$<br>( $\text{cm}^{-1}$ ) | $\omega_{\text{obs}}$<br>( $\text{cm}^{-1}$ ) |
|--|---|-----------------------|--|---|
| $\text{NaMnCrF}_6$<br>$\omega_{\text{Mn}} = 358 \text{ cm}^{-1}$ | Mn–F–Cr   | 132.1                 | 262  | 258   |
| $\omega_{\text{Cr}} = 538 \text{ cm}^{-1}$                       |  | 103.1                 | 404  | 358   |
|  |   | 102.2                 |  |   |

### III. Raman Data on Disordered Phases or Glasses

#### 1. The $\text{RbNiCrF}_6$ -type Pyrochlores

In the case of pyrochlore structure ( $\text{CsZnGaF}_6$ , (30)), all fluorine atoms are bounded either to  $\text{ZnF}_6$  or  $\text{GaF}_6$  octahedra (statistically disordered—Figs. 17 and 18, Table IV). Application of group theory shows that in the  $Fd3m$  space group, vibrations along the  $M-F$  bond are forbidden.

Two interpretations of the spectrum are possible, but both are inconsistent with the space group  $Fd3m$ :

—The statistical partition of Zn and Ga on the same site must result in many Zn–F–Ga connections in contradiction with the higher value found at  $604 \text{ cm}^{-1}$  (broad line) compared to  $538 \text{ cm}^{-1}$  for  $\omega_{\text{Cr}}$  in  $\text{NaMnCrF}_6$ . The broadening of the line could indicate both the cationic disorder and a notable amount of Ga–F–Ga connections.

—The  $604 \text{ cm}^{-1}$  vibration is a  $\omega_{\text{SS}}$  vibration indicating that the  $Fd3m$  space group is wrong as suggested by a previous EXAFS study (31). The lack of translational symmetry modifies the selection rules, allowing activity for normally forbidden modes.

#### 2. Three-Dimensional Transition Metal Fluoride Glasses

The “statistical” cationic distribution in the 16c site of  $\text{CsZnGaF}_6$  pyrochlore structure is probably a situation not far from that which exists in 3d transitional element

TABLE IV  
COMPARISON OF OBSERVED AND CALCULATED  
FREQUENCIES FOR BENDING MODES

| Crystal  | Bond    | $\theta$ ( $^\circ$ ) | $\omega_{\text{calc}}$<br>( $\text{cm}^{-1}$ ) | $\omega_{\text{obs}}$<br>( $\text{cm}^{-1}$ ) |
|--|---------|-----------------------|--|---|
| $\text{CsZnGaF}_6$<br>$\omega_{\text{Ga}} = 530 \text{ cm}^{-1}$<br>$\omega_{\text{Zn}} = 360 \text{ cm}^{-1}$ | Ga–F–Ga | 149.1                 | 369  | 385   |
|  | Ga–F–Zn | 137.8                 | 231  | 210   |
|  | Zn–F–Zn | 129.5                 | 220  |   |

<sup>a</sup> Estimated from  $r^{3/2} \cdot \omega = f(\sqrt{Z_m})$  curve.

fluoride glasses. Their structure can be described in two ways:

— $Mt^{II}F_6$  and  $Mt^{III}F_6$  octahedra are linked together essentially by corners but the

$Mt^{II}F_6$  octahedra are more connected than the  $Mt^{III}F_6$  octahedra; large cations ( $Pb^{2+}$ ,  $Ba^{2+}$  . . .) occupy the large holes of the tridimensional octahedral network very close to that of lacunary  $ReO_3$  type.

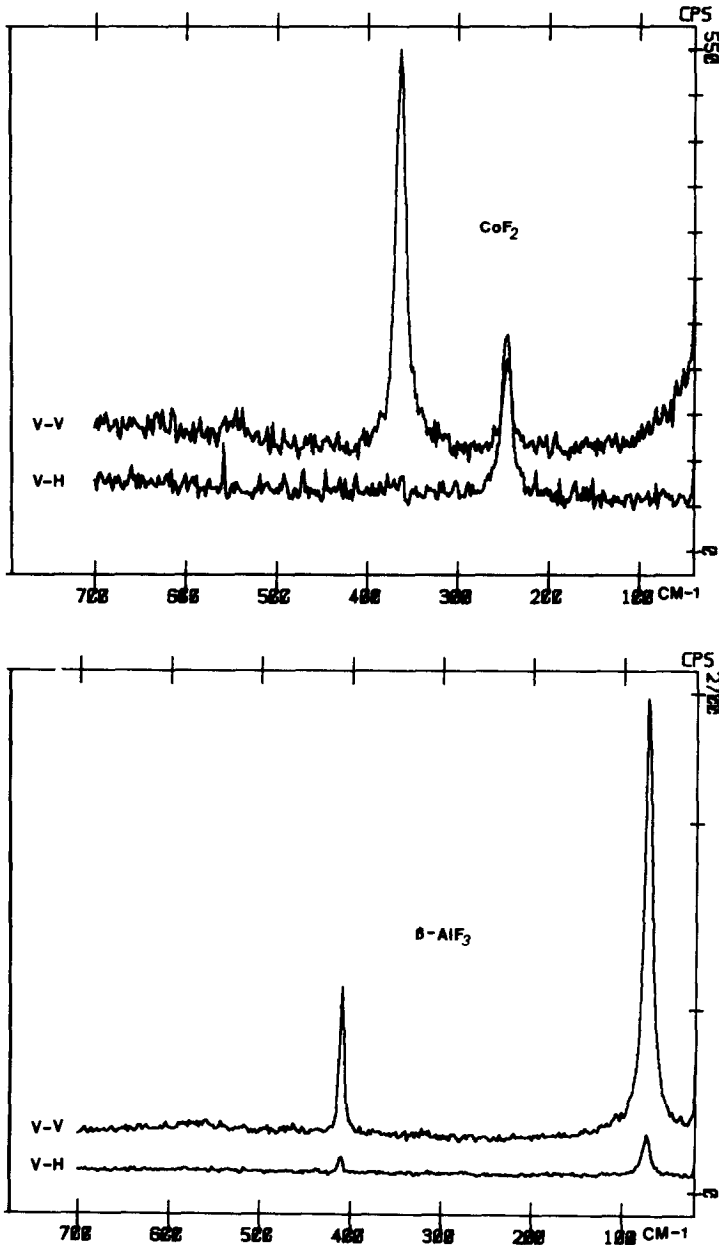


FIG. 16. Polarized spectra of  $CoF_2$ ,  $\beta-AlF_3$ , and  $NaMnCrF_6$ .

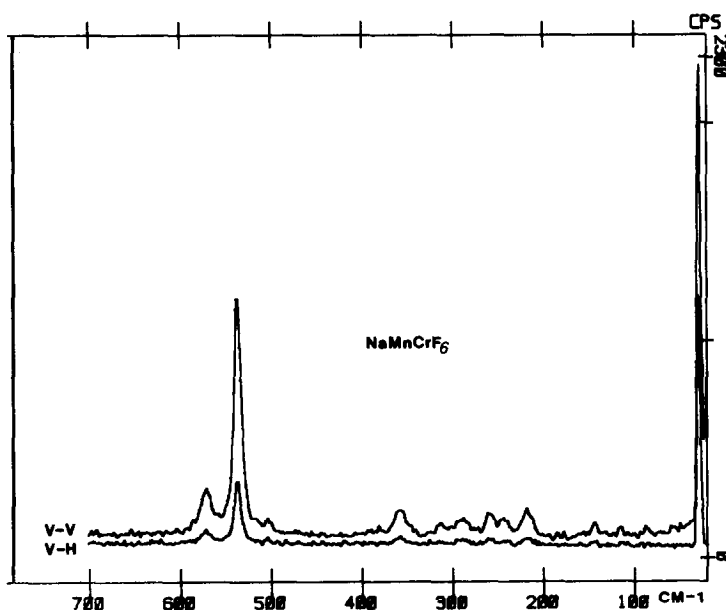


FIG. 16—Continued

—Three-dimensional transition metals fit the octahedral sites of a quasi-compact fluoride ion packing; the perturbation in the network is due to the insertion of the large cations ( $\text{Pb}^{2+}$ ,  $\text{Ba}^{2+}$  . . . , same size as  $\text{F}^-$ ) in the  $\text{F}^-$  packing.

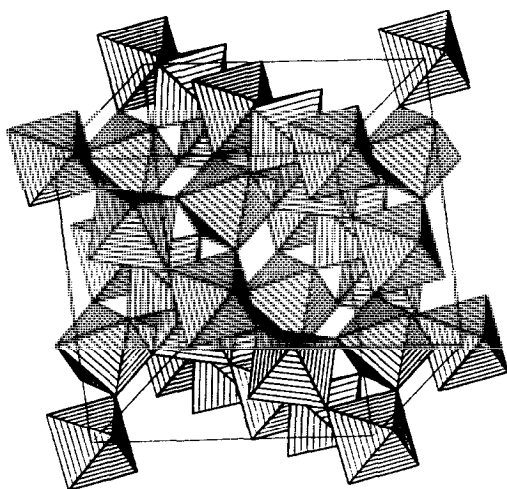
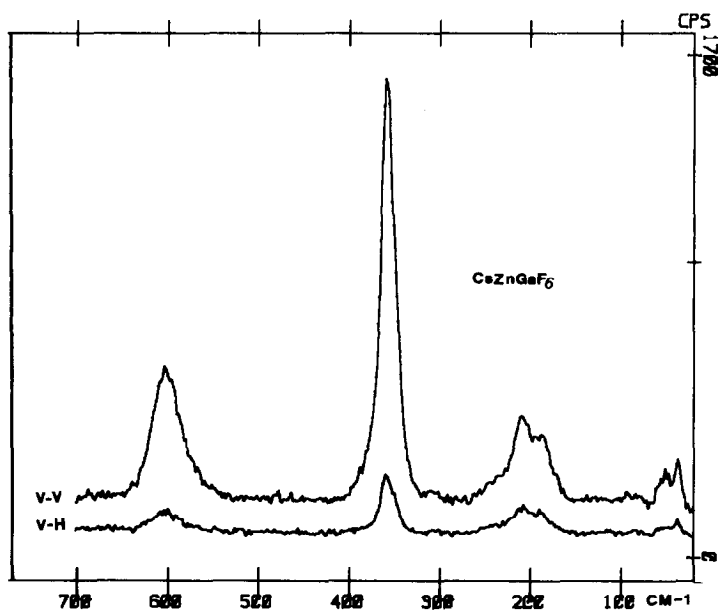
FIG. 17. Structure of  $\text{RbNiCrF}_6$ -type pyrochlore.

Figure 19 shows the average structure of TMFG.

Bose-Einstein (32) corrected Raman spectra of TMFG containing only  $M^{\text{III}}$  ions (Glass A) or  $M^{\text{II}}$  ions (Glass B) and both  $M^{\text{II}}$  and  $M^{\text{III}}$  ions (Glasses C and D) in six-fold coordination (from previous structural studies) are shown in Fig. 20. Glasses A, C, and D exhibit a narrow V-V polarized line in the range  $500\text{--}600\text{ cm}^{-1}$ :

—The replacement of  $\text{MnF}_2$  with  $\text{ZnF}_2$  (Glasses C, D) does not affect the  $560\text{ cm}^{-1}$  line leading us to the conclusion that this line is due to  $M^{\text{III}}\text{--F}$  stretching.

—We tried to compare the width (HWHM) of both this Raman line and the EXAFS radial distribution functions (RDF, (6)) in the case of the same glass (Glass D). Assuming again that the  $\omega_{\text{SS}}$  frequency can be written as:  $\text{constant} \cdot r^{-3/2}$ , we can see that  $\Delta\omega/\omega = 3/2 \Delta r/r$ ; this leads to  $\Delta r = 0.085\text{ \AA}$  (very close to the EXAFS value  $\Delta r = 0.08\text{ \AA}$ ).

FIG. 18. Polarized Raman spectrum of CsZnGaF<sub>6</sub>.

—This well-defined line, attributed to  $M^{III}$  cations, when associated with the broadened contributions of  $Pb^{2+}$  and  $M^{2+}$  in the low frequency range confirms that in these glasses the short-range order depends upon  $M^{III}F_6$  octahedra, while  $Pb^{2+}$  and  $M^{2+}$  could have the classical modifier behavior.

The comparison of variation of connecting scheme dependent criterion  $\Gamma = r^{3/2} \cdot \omega/\sqrt{q}$  with the glass composition (Table

V) leads to conclusions, consistent with the known structural models:

—*Glass A* ( $\Delta r = 0.086 \text{ \AA}$ ). The molar composition ratio  $In/(Pb + Ba) \approx 1$  implies the predominance of  $InF_6$  species and the possible existence of  $In-F-In$  connections; the  $\Gamma$  value is in favor of a monodimensional network.

—*Glass B* ( $\Delta r = 0.16 \text{ \AA}$ ). This glass (more unstable), contains only  $M^{II}F_6$  enti-

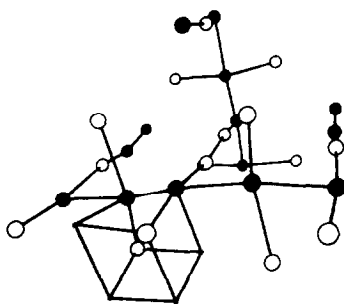


FIG. 19. Structural model for TMFG network: ●,  $M^{2+}$ ; ○,  $M^{3+}$ .

TABLE V  
VARIATION OF  $\Gamma = r^{3/2} \cdot \omega/\sqrt{q}$  WITH GLASS  
COMPOSITION

| Glass | Composition  | $\omega_{ss}$<br>( $cm^{-1}$ ) | $r(M-F)$<br>( $\text{\AA}$ ) | $\Gamma$ |
|-------|--|--------------------------------|------------------------------|----------|
| A     | 19.0PbF <sub>2</sub> -23.8BaF <sub>2</sub> -47.6InF <sub>3</sub><br>1.9AlF <sub>3</sub> -4.9SrF <sub>2</sub> -2.8YF <sub>3</sub> | 500                            | 2.02                         | 829      |
| B     | 20BaF <sub>2</sub> -50ZnF <sub>2</sub> -30YF <sub>3</sub>  | 410                            | 2.01 <sup>a</sup>            | 826      |
| C     | 35.3PbF <sub>2</sub> -23.5MnF <sub>2</sub> -34.3GaF <sub>3</sub><br>2.0AlF <sub>3</sub> -4.9YF <sub>3</sub>                      | 560                            | 1.90 <sup>a</sup>            | 847      |
| D     | 35.3PbF <sub>2</sub> -23.5ZnF <sub>2</sub> -34.3GaF <sub>3</sub><br>2.0AlF <sub>3</sub> -4.9YF <sub>3</sub>                      | 560                            | 1.90 <sup>a</sup>            | 847      |

<sup>a</sup> EXAFS results.

ties; the  $\omega_{SS}$  line found at  $410\text{ cm}^{-1}$  is large, indicative of the octahedra's distortion. The value of  $Zn/(Ba + Y)$ , related to the  $\Gamma$  value, predicts a situation analogous to that of Glass A.

—Glass C, D ( $\Delta r = 0.085\text{ \AA}$ ). According to the lower value of ratio  $Ga/(Pb + M^{II})$ , it can be expected that  $Ga-F-M^{II}$  connections become predominant; the  $\Gamma$  value indicates mostly isolated or "pseudo"-iso-

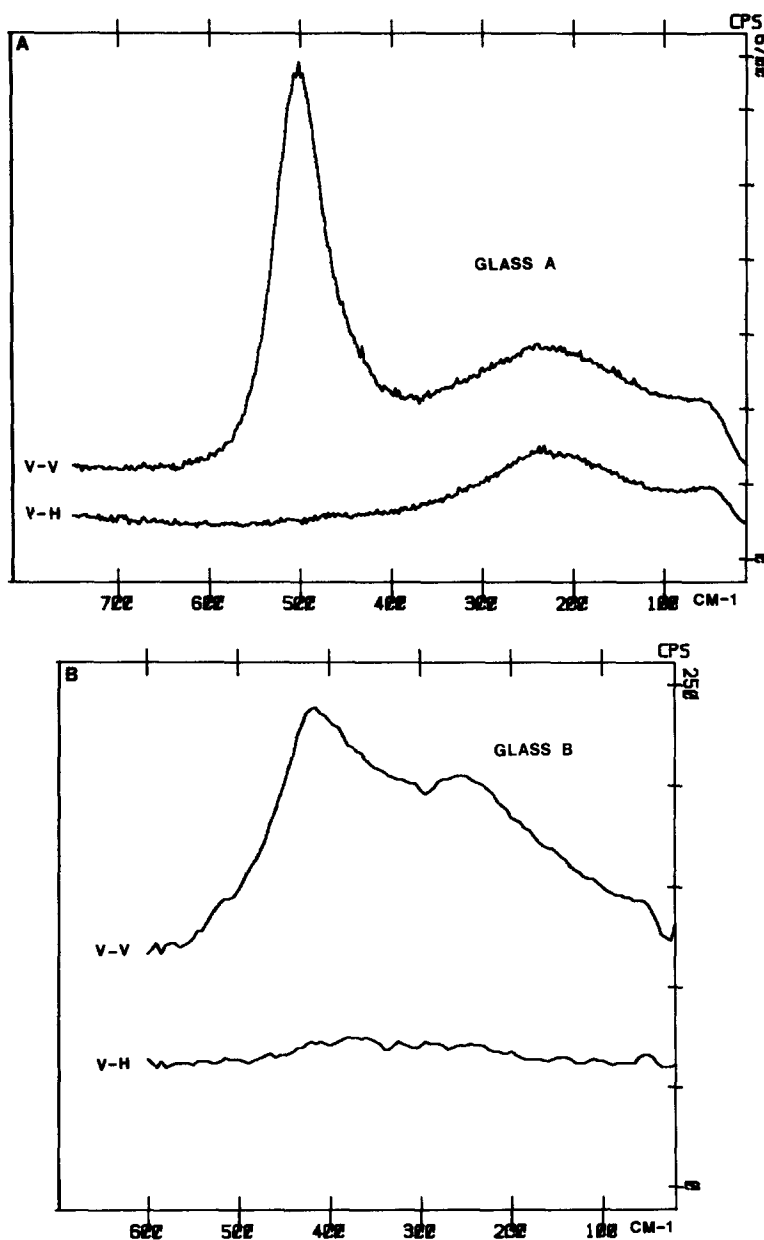


FIG. 20. V-V and V-H Bose-Einstein corrected spectra of glasses A, B, C, and D. (For glass composition refer to Table V.)

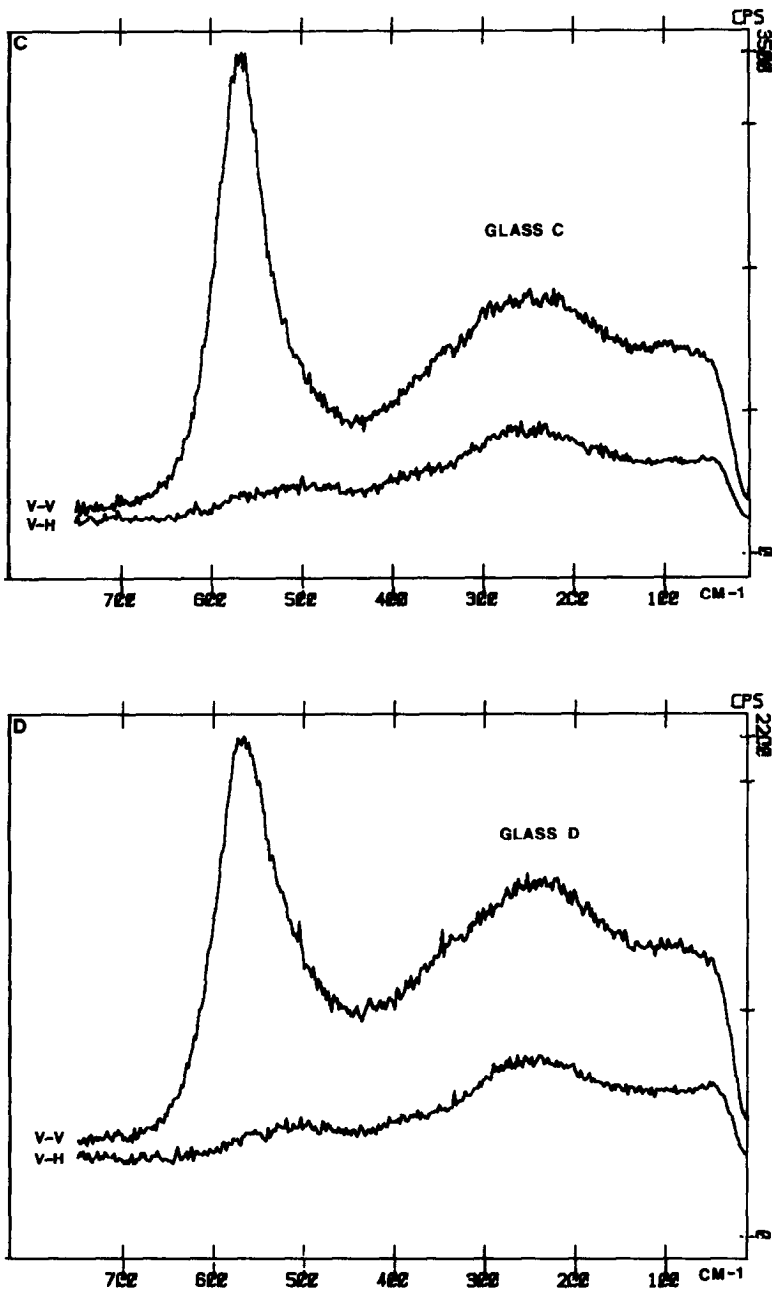


FIG. 20-Continued

lated  $M^{\text{III}}\text{F}_6$  octahedra. We already noticed that in  $\text{NaMnCrF}_6$ , Mn has no effect on  $M^{\text{III}}\text{-F}$   $\omega_{\text{SS}}$  vibration. This view is consis-

tent with the model of alternated  $\text{Ga-M}^{\text{II}}$  chains based on NMR studies (8); however, we cannot exclude the existence of the

Ga-F-Ga connection since the  $604\text{ cm}^{-1}$  frequency found in the pyrochlore is similar to that value.

#### IV. Conclusion

Raman spectra recording of small crystals (down to 0.1 mm) was made possible thanks to a micro-Raman spectrometer. Study of single crystals of octahedrally coordinated fluorides has shown that the symmetric stretching frequency  $\omega_{SS}$  mainly depends on the oxidation number of the metal and then on the degree of connectivity; but the case of three-dimensional structures is more complex.

TMFG study shows unambiguously that the less-distorted octahedra are  $M^{III}F_6$ , with predominance of the  $\omega_{SS}$  vibration of  $M^{III}-F$  bonds. The short-range order is mainly due to trivalent metal octahedra; the structural view is consistent with that given previously by other studies.

#### Acknowledgments

We thank G. Courbion and J. L. Fourquet for providing us with some of the single crystals and A. Bulou for helpful discussions.

#### References

1. R. M. ALMEIDA (Ed.), *VILAMOURA, NATO ASI Ser. E: Appl. Sci.* **123** (1986).
2. M. MONERIE, *New Materials for Optical Waveguides*, SPIE, Vol. 799, pp. 123-130 (1987).
3. A. LE BAIL, C. JACOBONI, AND R. DE PAPE, *J. Solid State Chem.* **48**, 168-175 (1983).
4. A. LE BAIL, C. JACOBONI, AND R. DE PAPE, *J. Non-Cryst. Solids* **74**, 205-212 (1985).
5. A. LE BAIL, C. JACOBONI, AND R. DE PAPE, *Mater. Sci. Forum* **6**, 441-448 (1985).
6. A. LE BAIL, C. JACOBONI, AND R. DE PAPE, *J. Solid State Chem.* **52**, 32-44 (1984).
7. G. COURBION, J. GUERY, A. LE BAIL, AND C. JACOBONI, *Mater. Sci. Forum* **6**, 739-742 (1985).
8. C. DUPAS, K. LE DANG, J. P. RENARD, P. VEILLET, J. P. MIRANDAY, AND C. JACOBONI, *J. Phys.* **42**, 1345-1350 (1981).
9. J. P. RENARD, J. P. MIRANDAY, AND F. VARRET, *Solid State Commun.* **35**, 41-44 (1980).
10. J. NOUET, C. JACOBONI, G. FERREY, J. Y. GERARD, AND R. DE PAPE, *J. Cryst. Growth* **8**, 94-98 (1970).
11. M. LEBLANC, G. FERREY, AND R. DE PAPE, *Mater. Res. Bull.* **19**, 1581-1590 (1984).
12. N. AURIAULT, J. GUERY, A. M. MERCIER, C. JACOBONI, AND R. DE PAPE, *Mater. Res. Bull.* **20**, 309-314 (1985).
13. A. LEBLE, J. C. FAYET, AND C. JACOBONI, *C. R. Acad. Sci.* **T277**, 647-650 (1973).
14. K. KNOX AND D. W. MITCHELL, *J. Inorg. Nucl. Chem.* **21**, 253 (1961).
15. J. L. FOURQUET, F. PLET, AND R. DE PAPE, *Rev. Chim. Miner.* **18**, 19-26 (1981).
16. C. JACOBONI, R. DE PAPE, M. POULAIN, J. Y. LE MAROUILLE, AND D. GRANDJEAN, *Acta Crystallogr. Sect. B* **30**, 2688 (1974).
17. J. L. FOURQUET, F. PLET, G. COURBION, AND R. DE PAPE, *Rev. Chim. Miner.* **16**, 490-500 (1979).
18. J. L. FOURQUET, F. PLET, AND R. DE PAPE, *Acta Crystallogr. Sect. B* **36**, 1997-2000 (1980).
19. C. JACOBONI, A. LEBLE, AND J. J. ROUSSEAU, *J. Solid State Chem.* **36**, 297-304 (1981).
20. G. COURBION, C. JACOBONI, AND R. DE PAPE, *Acta Crystallogr. Sect. B* **32**, 3190-3193 (1976).
21. R. W. G. WYCKOFF, "Crystal Structures," Vol. 1, p. 251, Interscience, New York (1965).
22. A. LE BAIL, C. JACOBONI, M. LEBLANC, R. DE PAPE, H. DUROY, AND J. L. FOURQUET, *J. Solid State Chem.* **77**, 96-101 (1988).
23. G. COURBION, C. JACOBONI, AND R. DE PAPE, *Acta Crystallogr. Sect. B* **33**, 1405-1408 (1977).
24. A. BULO, M. ROUSSEAU, J. NOUET, P. L. LOYZANCE, R. MOKHLISSE, AND M. COUZI, *J. Phys. C: Solid State Phys.* **16**, 4527-4537 (1983).
25. A. BULO, M. ROUSSEAU, J. NOUET, AND B. HENNION, submitted for publication.
26. M. ROUSSEAU, J. Y. GESLAND, J. JUILLARD, J. NOUET, AND A. ZAREMBOVITCH *Phys. Rev. B* **12**(4), 1579-1590 (1975).
27. L. M. TOTH, A. S. QUIST, AND G. E. BOYD, *J. Phys. Chem.* **77**, 11, 1384 (1973).
28. R. M. ALMEIDA, *J. Chem. Phys.* **78**, 11, 6502-6511 (1983).
29. A. BULO, Thèse de Doctorat d'Etat, Paris VI-Le Mans (1985).
30. D. BABEL, *Z. Anorg. Allg. Chem.* **387**, 161 (1972).
31. A. LE BAIL, C. JACOBONI, AND R. DE PAPE, *J. Solid State Chemistry* **61**, 188-196 (1986).
32. G. E. WALRAFEN, M. S. HOKMABADI, S. GUHA, AND P. N. KRISHNAN, *J. Chem. Phys.* **83**, 4427-4443 (1985).